East European Journal of Physics. 3. 498-504 (2026)
DOI:10.26565/2312-4334-2026-3-45 ISSN 2312-4334

ELECTRON STATES IN FIVE-LAYER SEMICONDUCTOR STRUCTURES. PART 2

R.Ya. Rasulov, V.R. Rasulov, I.A. Muminov*, M.A. Mamatova, F.U. Raxmatullayeva, S.X. Muxammadaminov
Fergana State University, Murabbiylar St., 19, Fergana, 150100, Uzbekistan
**Corresponding Author e-mail: islommuminov2207@gmail.com*
Received January 13, 2026; revised May 5, 2026; in final form June 24, 2026; accepted August 25, 2026

Transcendental equations for determining the electron energy spectrum in a five-layer semiconductor structure with a potential barrier located at its center have been derived and analyzed for different energy ranges. It is shown that the origin of the energy-level shift is associated with the dependence of the electron Hamiltonian not only on the potential energy but also on the kinetic energy, which is governed by the effective masses of electrons in each layer of the structure. Changes in the electron energy spectrum of a five-layer semiconductor structure whose layers have different values of physical quantities characterizing the band and geometrical parameters of the sample as a function of temperature have been analyzed.
Keywords: *Five-layer semiconductor structure; Coupled quantum wells; Potential barrier; Electron energy spectrum; Transcendental quantization equations; Effective mass mismatch; Bastard boundary conditions; Temperature dependence; Kane model; resonant tunneling structures*

INTRODUCTION

The current stage of development of solid-state physics is characterized by the fact that the primary objects of research are increasingly not bulk semiconductor crystals, but thin films, multilayer thin-film structures, conducting wires, and crystallites [1–4]. The small dimensions of these structures in a certain direction, comparable to the de Broglie wavelength, lead—according to the laws of quantum mechanics—to a modification of the energy spectrum of charge carriers. The spectrum becomes discrete for motion along the axis in which the motion is confined. The presence of such "size" quantization, under certain conditions, can significantly affect the physical properties of the quantum-confined structures under consideration, giving rise to a set of unique properties that differ from those of single-crystal semiconductors [2–9].

The experience accumulated to date and the advances in epitaxial growth techniques make it possible to fabricate more complex heterocompositions containing semiconductor layers with a complex potential profile. From this perspective, the investigation of the particle energy spectrum in coupled quantum wells is of considerable interest, since in such systems it is possible to purposefully control the energy spectrum and electron scattering rates by changing not only the shape of the quantum well but also the coupling between the wells. Structures with coupled quantum wells have become the basis of many electronic and optoelectronic devices [1–4]. On the basis of these multilayer semiconductor structures, infrared (IR) lasers, IR radiation detectors, nonlinear optical elements, and high-speed transistors have been developed [1–4].

Due to the development of nanoelectronics, such problems have been revisited, and solutions have been obtained for a number of potential profiles of complex form [3, 5–16]. However, quantum-mechanical problems associated with electron motion in a multilayer semiconductor structure of arbitrary profile require treatment within the framework of perturbation theory. Therefore, below we calculate the electron energy spectrum in multilayer structures and its dependence on the sample temperature.

METHODS

Electron energy spectrum in multilayer semiconductor structures. To clarify how the shape, height, and spatial position of a potential barrier that divides a quantum well affect the resulting energy spectrum, we consider a five-region model of a layered semiconductor heterostructure, schematically shown in Fig. 1. Such a representation makes it possible to capture the essential features of quantum confinement and interlayer coupling in systems where the potential profile changes stepwise across the interfaces.

In this model, m_i denotes the effective mass of charge carriers in the i-th layer material, reflecting the layer-dependent kinetic-energy contribution to the electron Hamiltonian. The parameters U_1 and U_2 specify the positions of the conduction-band edges in the corresponding layers and therefore define the depth of the quantum well and the barrier height within the structure. The geometrical characteristics of the central part of the heterostructure are determined by the nanolayer thicknesses d_2, d_3, and d_4 which form the coupled-well region and control both the degree of confinement and the tunneling interaction between spatially separated parts of the well. This set of band and geometrical parameters

Cite as: R.Ya. Rasulov, V.R. Rasulov, I.A. Muminov, M. A. Mamatova, F.U. Raxmatullayeva, S.X. Muxammadaminov, East Eur. J. Phys. 3, 498 (2026), https://doi.org/10.26565/2312-4334-2026-3-45

provides a convenient basis for analyzing the formation and evolution of discrete electron states in multilayer quantum-well systems. As is known, the behavior of electrons in each region of the structure is described by the Schrödinger equation:

$$\frac{\hbar^2}{2m_i^*}\cdot\frac{\partial^2\psi_i(x)}{\partial x^2}+(E-U_i)\psi_i=0, \tag{1}$$

where $i=1,2,\ldots,5$ are the layer indices of the structure.

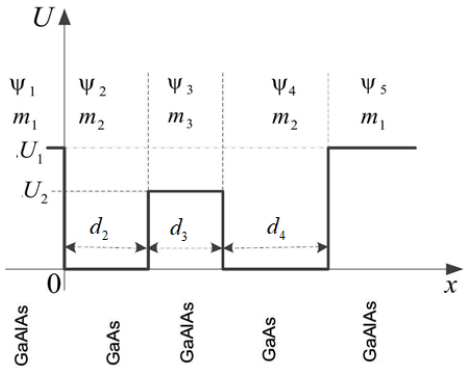

Figure 1. Conduction-band edge profile in a layered semiconductor structure.

Equation (1) is to be understood as the layer-wise (piecewise) form of the more general one-dimensional effective-mass Schrödinger equation with position-dependent mass $m^*(x)$, namely

$$-\left(\frac{\hbar^2}{2}\right)\left(\frac{d}{dx}\right)\left[\left(\frac{1}{m^*(x)}\right)\left(\frac{d\psi(x)}{dx}\right)\right]+U(x)\,\psi(x)=E\,\psi(x). \tag{1a}$$

In equation (1a) the operator $1/m^*(x)$ is placed between the two derivatives in order to preserve the Hermiticity of the kinetic-energy operator when $m^*(x)$ is piecewise-constant [19, 20]. Within each layer $m^*(x)$ is constant and (1a) reduces to (1); the matching conditions at the heterointerfaces follow automatically from the integration of (1a) across each interface and are precisely the *Bastard (BenDaniel–Duke) boundary conditions*: continuity of the envelope function $\psi_{\mathrm{n}}(x_{\mathrm{i}})=\psi_{\mathrm{n+1}}(x_{\mathrm{i}})$ and continuity of the probability current $(1/m_{\mathrm{n}})d\psi_{\mathrm{n}}/dx=(1/m_{\mathrm{n+1}})d\psi_{\mathrm{n+1}}/dx$ evaluated at every interface $x_{\mathrm{i}}\in\{0,d_2,d_2+d_3,d_2+d_3+d_4\}$. The system (4) given below is the explicit form of these matching conditions. The Bastard condition has been recently used by the present authors in the analysis of asymmetric multilayer semiconductor structures [24] and is a standard ingredient in modern envelope-function calculations for resonant-tunnelling heterostructures [21–23].

The values of the potential energies and effective masses in expression (1) are specified as follows:

$$U_i=\begin{cases}U_1, x\le 0, x>d_2+d_3+d_4,\\ 0, 0<x\le d_2, d_2+d_3<x\le d_2+d_3+d_4,\\ U_2, d_2<x\le d_2+d_3,\end{cases} \tag{2}$$

$$m_i^*=\begin{cases}m_1, x\le 0, x>d_2+d_3+d_4,\\ m_2, 0<x\le d_2, d_2+d_3<x\le d_2+d_3+d_4,\\ m_3, d_2<x\le d_2+d_3.\end{cases} \tag{3}$$

A remark on notation. Equation (3) lists only three distinct effective masses (m_1, m_2, m_3) because the structure shown in Fig. 1 is left–right symmetric ($m_5=m_1,\ m_4=m_2$). For the *general (asymmetric) case*, treated in equations (4)–(6) below, the corresponding extension reads

$$m_i^*=m_1\,(x\le 0);\ m_2\,(0<x\le d_2);\ m_3\,(d_2<x\le d_2+d_3);$$

$$m_4\,(d_2+d_3<x\le d_2+d_3+d_4);\ m_5\,(x>d_2+d_3+d_4). \tag{3a}$$

The wave numbers in the four inner and outer regions are then defined accordingly: $k_1=[2m_1(U_1-E)/\hbar^2]^{1/2}$, $k_2=(2m_2E/\hbar^2)^{1/2}$, $k_3=[2m_3(U_2-E)/\hbar^2]^{1/2}$, $k_4=(2m_4E/\hbar^2)^{1/2}$, $k_5=[2m_5(U_1-E)/\hbar^2]^{1/2}$. The symmetric structure of Fig. 1 corresponds to the special case $m_4=m_2, m_5=m_1$ (and consequently $k_4=k_2, k_5=k_1$); the formulas (4), (5), and (6) below are written in this general form, so that they remain valid for asymmetric structures with all five effective masses different.

The solution of the Schrödinger equation (for $E < U_1, U_2$) for each of the five regions is written as:

$$\begin{cases} \psi_1 = A_1 \cdot \exp(k_1 x) \\ \psi_2 = A_2 \cdot \cos(k_2 x) + B_2 \cdot \sin(k_2 x) \\ \psi_3 = A_3 \cdot \mathrm{ch}\big(k_3(x-d_3)\big) + B_3 \cdot \mathrm{sh}\big(k_3(x-d_3)\big) \\ \psi_4 = A_4 \cdot \cos\big(k_2(x-d_2-d_3)\big) + B_4 \cdot \sin\big(k_2(x-d_1+d_2)\big) \\ \psi_5 = B_5 \cdot \exp\big(-k_1(x-d_1-d_2-d_3)\big) \end{cases},$$

here, $k_1 = \sqrt{2m_1^*\hbar^{-2}|U_1 - E|},\ k_2 = \sqrt{2m_2^*\hbar^{-2}E},\ k_3 = \sqrt{2m_3^*\hbar^{-2}|U_2 - E|}$.

The Bastard boundary conditions, which follow from the requirements of continuity of the wave function and the probability current density, form the following system of equations:

$$\begin{cases} A_1 - A_2 = 0 \\ \tilde{k}_1 A_1 - \tilde{k}_2 B_2 = 0 \\ A_2\cos(k_2 d_2) + B_2\sin(k_2 d_2) - A_3 = 0 \\ -\tilde{k}_2 A_2\sin(k_2 d_2) + \tilde{k}_2 B_2\cos(k_2 d_2) - \tilde{k}_3 B_3 = 0 \\ A_3\mathrm{ch}(k_3 d_3) + B_3\mathrm{sh}(k_3 d_3) - A_4 = 0 \\ \tilde{k}_3 A_3\mathrm{sh}(k_3 d_3) + \tilde{k}_3 B_3\mathrm{ch}(k_3 d_3) - \tilde{k}_4 B_4 = 0 \\ A_4\cos(k_4 d_4) + B_4\sin(k_4 d_4) - B_5 = 0 \\ -\tilde{k}_4 A_4\sin(k_4 d_4) + \tilde{k}_4 B_4\cos(k_4 d_4) + \tilde{k}_5 B_5 = 0 \end{cases} \tag{4}$$

The resulting system (4) has nontrivial solutions with respect to the unknown energy values only when the determinant formed from the coefficients of the unknowns is equal to zero. As a result, we obtain an expression for determining the electron energy, which is convenient to present in the form:

$$\big[-\tilde{k}_2\big(\tilde{k}_1 - \tilde{k}_3\big)\cos(k_2 d_2) + \big(\tilde{k}_1\tilde{k}_3 + \tilde{k}_2^2\big)\sin(k_2 d_2)\big]\big[\tilde{k}_4\cos(k_4 d_4) + \tilde{k}_5\sin(k_4 d_4)\big]\big[\tilde{k}_4\mathrm{sh}(k_3 d_3) - \tilde{k}_3\mathrm{ch}(k_3 d_3)\big] = 0. \tag{5}$$

where $\tilde{k}_i = \frac{k_i}{m_i}$. Similarly, by solving the corresponding boundary-value problem, we obtain an expression that can be used to determine the energy spectrum for bound states when $U_1 \geq E > U_2$.

$$\big[\tilde{k}_2^2\big(\tilde{k}_3^2 - \tilde{k}_1^2\big) + \big(\tilde{k}_1^2\tilde{k}_3^2 - \tilde{k}_2^4\big)\mathrm{tg}(k_2 d_4)\big]\mathrm{tg}(k_3 d_3) + 2\tilde{k}_1\tilde{k}_2^2\tilde{k}_3 \cdot [\mathrm{tg}(k_2 d_2)\mathrm{tg}(k_2 d_4) - 1] +$$

$$+\tilde{k}_2\big[\tilde{k}_3\big(\tilde{k}_2^2 - \tilde{k}_1^2\big) + \tilde{k}_1\big(\tilde{k}_3^2 + \tilde{k}_2^2\big)\mathrm{tg}(k_3 d_3)\big][\mathrm{tg}(k_2 d_2) + \mathrm{tg}(k_2 d_4)] = 0.$$

(6)

For a well with a high potential barrier U_1($U_1 \gg U_2$), one can use the model of an infinitely deep well. In this case, the energy spectrum is determined by a transcendental equation which, for $E < U_2$, takes the form:

$$\big[\tilde{k}_2^2 + \tilde{k}_3^2\mathrm{tg}(k_2 d_2)\mathrm{tg}(k_2 d_4)\big]\mathrm{th}(k_3 d_3) + \tilde{k}_2\tilde{k}_3[\mathrm{tg}(k_2 d_2) + \mathrm{tg}(k_2 d_4)] = 0,$$

and for $E > U_2$:

$$\big[\tilde{k}_2^2 - \tilde{k}_3^2\mathrm{tg}(k_2 d_2)\mathrm{tg}(k_2 d_4)\big]\mathrm{tg}(k_3 d_3) + \tilde{k}_2\tilde{k}_3[\mathrm{tg}(k_2 d_2) + \mathrm{tg}(k_2 d_4)] = 0.$$

In the case $E < U_2$ for an infinitely deep well, the expressions for the coefficients defining the wave function, up to the normalization factor B, take the form:

$$A_1 = A_2 = B_5 = 0, B_2 = B, A_3 = B \cdot \sin(k_2 d_2), B_3 = B\frac{\tilde{k}_2}{\tilde{k}_3}\cos(k_2 d_2),$$

$$A_4 = B\left[\frac{\tilde{k}_2}{\tilde{k}_3}\cos(k_2 d_2)\mathrm{sh}(k_3 d_3) - \sin(k_2 d_2)\mathrm{ch}(k_3 d_3)\right],$$

$$B_4 = -B\left[\frac{\tilde{k}_2}{\tilde{k}_3}\cos(k_2 d_2)\mathrm{sh}(k_3 d_3) - \sin(k_2 d_2)\mathrm{ch}(k_3 d_3)\right]\mathrm{ctg}(k_2 d_4). \tag{7}$$

The obtained energy-quantization conditions make it possible to analyze the influence of the position and width of the barrier separating the quantum well on the energy spectrum of charge carriers in nanoelectronic devices based on

heterojunctions and superlattice structures with a variable doping profile. The expressions that determine the wave function in the quantum well also enable one to evaluate electron localization as a function of the potential landscape and the doping profile.

For a relatively small barrier height compared with the depth of the main part of the well ($U_2 \ll U_1$), the relative shift of the ground and first excited state energies can be qualitatively explained on the basis of perturbation theory [5,10], as was done in [6] for a well with an energy dip. In the first approximation, for a barrier of width d_3 and height U_2 located at the center of an infinitely deep quantum well of width $d_2 + d_3$, we obtain:

$$\delta E_1^{(1)} = U_2\left[\frac{d_2}{d_2+d_3} + \frac{1}{\pi}\sin\left(\pi\frac{d_2}{d_2+d_3}\right)\right], \delta E_2^{(1)} = U_2\left[\frac{d_2}{d_2+d_3} - \frac{1}{2\pi}\sin\left(\frac{2\pi d_2}{d_2+d_3}\right)\right]. \quad (8)$$

As follows from (8) and Fig. 2, as d_3/d_2 and U_2 increase, the energy levels in the quantum well shift upward, both for the ground state and for the excited state. Obviously, a more detailed explanation of the shifts of the ground and excited states requires taking into account the difference in effective masses; accordingly, within the infinite-wall quantum-well model we obtain:

$$\delta E_n^{(1)} = \left(\frac{\pi n^2\hbar^2}{2(d_2+d_3)^2}\left(\frac{1}{m_3} - \frac{1}{m_2}\right) + U_2\right)\left(\frac{d_2}{d_2+d_3} - \frac{(-1)^n}{n\pi}\sin\left(\frac{2\pi n d_2}{d_2+d_3}\right)\right). \quad (9)$$

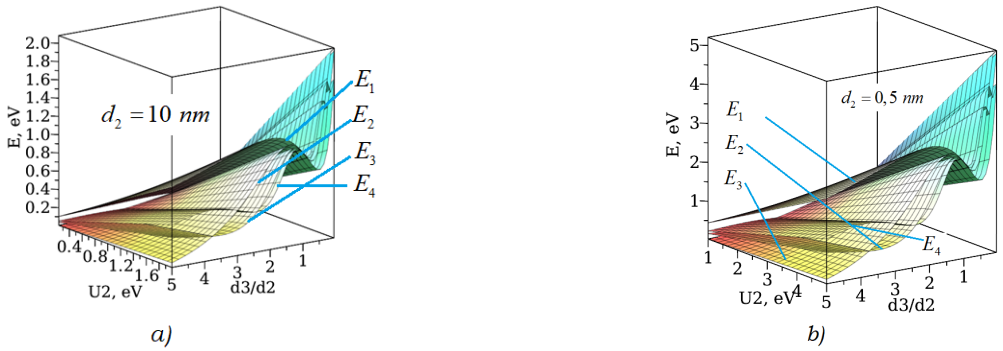

Figure 2. Dependences of the energies $E_n = \delta E_n^{(1)}(n = 1,2,3,4)$ on the depth of the potential dip (U_2) and on the thickness ratio of the 3rd and 2nd layers (d_3/d_2) for two values: $d_2 = 10$ nm and $d_2 = 0.5$ nm.

From the plots illustrating the dependence of $\delta E_n^{(1)}$ for four values $E_n(n = 1,2,3,4)$ on the thicknesses of the 2nd and 3rd layers, as well as on the ratio of their effective masses, it can be seen that the energy $\delta E_n^{(1)}$ and the energies $E_n(n = 1,2,3,4)$ depend significantly on the ratios d_2/d_3 and m_2/m_3. That is, whether the energies E_1, E_2, E_3, E_4 are larger or smaller than one another is determined by the layer thicknesses of the structure and by the relative values of the electron effective masses in the layers. This circumstance can be explained by the complexity of the dependence of the eigenenergy in the considered problem on the layer thicknesses of the structure and on the effective masses of the charge carriers.

This is related to the fact that the electron Hamiltonian [2,3] in a potential well with a barrier differs not only by the potential-energy operator but also by the kinetic-energy operator (due to the difference in effective masses in different layers of the structure).

Calculations show that modifying the potential landscape of a simple potential well by introducing a barrier of height U_2 should lead to an increase in the energy levels; simultaneously, the difference in kinetic energies for $m_3 < m_2$ also contributes to an upward shift of the levels, whereas for $m_3 > m_2$, on the contrary, it leads to a decrease in the energies. Note that within the first-order approximation of perturbation theory, it is possible to qualitatively explain the physical origin of the energy-level shifts only for small values of $d_3/(d_2 + d_3 + d_4)$; as the barrier width increases, higher-order approximations must be taken into account.

In the following calculations, the temperature dependence of the band gap by Vurgaftman

$$E_g(T) = E_g(T = 0) - \gamma_T T^2/(T + T_V), \quad (10)$$

and by Passler

$$E_g(T) = E_g(T = 0) - \frac{1}{2}\alpha\Theta_p\left[\left(1 + \left(2T/\Theta_p\right)^p\right)^{1/p} - 1\right]. \quad (11)$$

We consider the relations presented by Passler in this case, according to the multi-zone Kane model, the effective mass of an electron in the conduction band (m_c) is also temperature-dependent and is expressed as follows:

$$m_0/m_c = \{1 + 2F + E_P(E_g + 2\Delta_{SO}/3)/[3E_g(E_g + \Delta_{SO})]\}, \quad (12)$$

Here, $E_{g0} = E_g(T = 0)$. For the semiconductors used in the numerical calculations, the numerical values of the parameters α, Θ_p, and p were taken from Vurgaftman and Passler. In particular,

for $AlAs$: $E_g(T = 0\,K) = 3.099\,eV$, $E_p = 21.1\,eV$, $\alpha = 0.362\,meV/K$, $\Theta_p = 218\,K$, $\Delta_{so} = 0.28\,eV$, $F = -0.48, \gamma_T = 0.885\,meV/K$, $\beta = 530\,K$, $p = 2.32$;

for $InAs$: $\Theta_p = 143\,K$, $E_g(T = 0\,K) = 0.417\,eV$, $\gamma_T = 0.276\,meV/K$, $\beta = 93\,K$, $\alpha = 0.281\,meV/K$, $p = 2.10$, $E_p = 21.5\,eV$, $\Delta_{so} = 0.39\,eV$, $F = -2.90$.

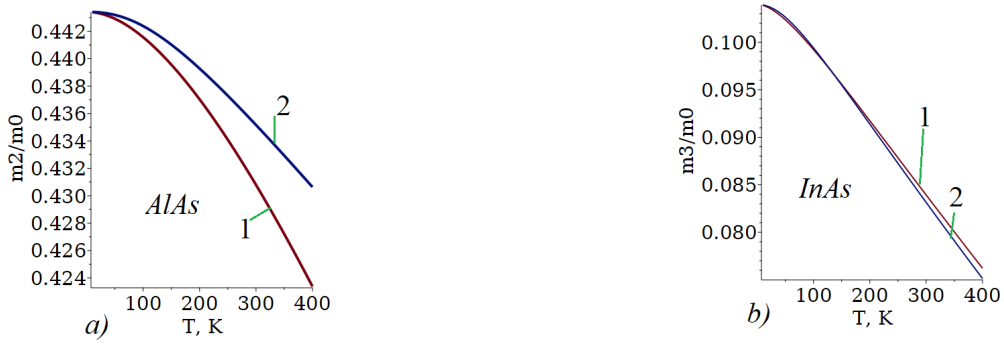

Figure 3. Temperature dependence of the electron effective mass in two semiconductors, calculated using the Vurgaftman formula (curve 2) and the Passler formula (curve 1).

From the temperature dependence of the electron effective mass in the two semiconductors (Fig. 3), it can be seen that the effective mass is almost independent of the choice between the Vurgaftman and Passler formulas, which is reflected in the subsequent results. From Figs. 4–5, it is evident that as the temperature increases, the numerical value of $E_n = \delta E_n^{(1)}$ $(n = 1,2,3,4)$ increases, but does not depend on the specific form of the temperature dependence.

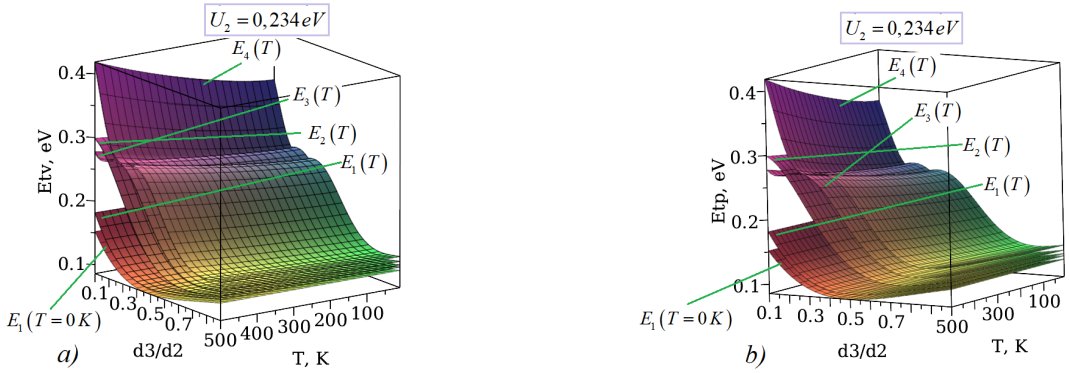

Figure 4. Dependences of the energies $E_n = \delta E_n^{(1)}$ $(n = 1,2,3,4)$ on temperature and on the thickness ratio of the 3rd and 2nd layers (d_3/d_2). Curves in (a) were calculated using the Vurgaftman formula, and in (b) using the Passler formula for $U_2 = 0.234$ eV, $d_2 = 10$ nm, $m_2 = 0.15\,m_0$, $m_3 = 0.026\,m_0$, where m_0 is the free-electron mass.

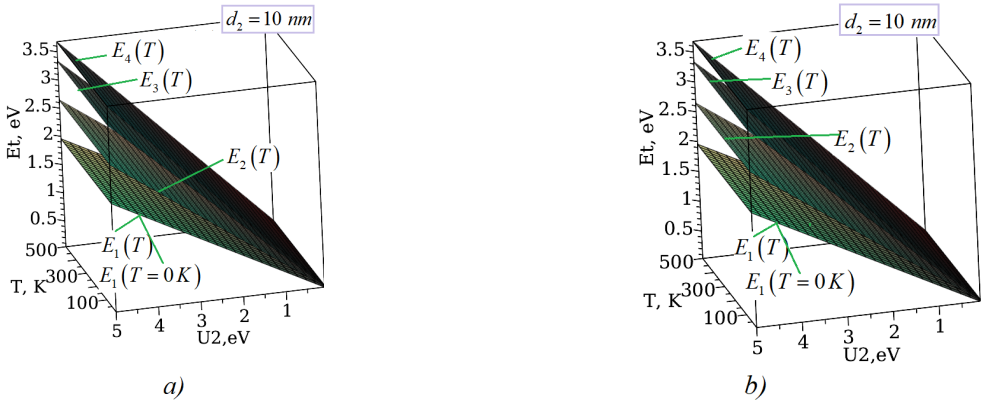

Figure 5. Dependences of the energies $E_n = \delta E_n^{(1)}$ $(n = 1,2,3,4)$ on temperature and on U_2. Curves in (a) were calculated using the Vurgaftman formula, and in (b) using the Passler formula, where $d_3 = d_2 = 10$ nm, $m_2 = 0.15\,m_0$, and $m_3 = 0.026\,m_0$.

Thus, the evolution of the electron energy spectrum in a five-layer semiconductor structure has been analyzed for the case where the individual layers differ in the key physical quantities that determine both the band alignment and the geometrical configuration of the sample. The obtained quantization conditions explicitly demonstrate that the positions of the discrete energy levels are governed not only by the potential profile (barrier height, width, and location), but also by the layer-dependent effective masses that enter the kinetic-energy operator and, therefore, shift the spectrum through mass mismatch at the interfaces.

CONCLUSIONS

The derived analytical expressions together with the numerical results indicate that the infinitely deep quantum-well approximation can serve only as a qualitative model for complex-profile wells when the confinement is sufficiently strong, i.e., for wells of relatively large depth. For shallower wells or for structures with pronounced internal barriers and material-parameter discontinuities, accurate determination of the level positions requires the full transcendental quantization relations obtained from the boundary-value problem. These relations, which account for the realistic potential landscape and the effective-mass discontinuities, provide a practical basis for predicting and tailoring the electron spectrum and carrier localization, and can therefore be applied to the design and optimization of resonant-tunneling heterostructures and related high-speed, low-inertia nanoelectronic devices.

ORCID

Rustam Y. Rasulov, https://orcid.org/0000-0002-5512-0654; **Voxob R. Rasulov,** https://orcid.org/0000-0001-5255-5612
Islom A. Muminov, https://orcid.org/0000-0002-2622-6097; **Maxliyo A. Mamatova,** https://orcid.org/0000-0001-6980-9877

REFERENCES

[1] Z.D. Kvon, "Semiconductor quantum wells and nanostructures," Nanomaterials, **13**(13), 1924 (2023). https://doi.org/10.3390/nano13131924
[2] E.L. Ivchenko, and G. E. Pikus, *Superlattices and Other Heterostructures. Symmetry and Optical Phenomena*. (Springer, Berlin, 1995).
[3] E. L. Ivchenko, *Optical Spectroscopy of Semiconductor Nanostructures*, (Alpha Science, Harrow (UK), 2005).
[4] H. Xu, M.K. Akbari, and S. Zhuiykov, "2D semiconductor nanomaterials and heterostructures: controlled synthesis and functional applications," Nanoscale Research Letters, **16**(1), 94 (2021). https://doi.org/10.1186/s11671-021-03551-w
[5] R.Ya. Rasulov, V.R. Rasulov, B.B. Akhmedov, I.A. Muminov, and K.K. Urinova, "Dimensional quantization in InSb and GaAs in three-zone model," Journal of Physics: Conference Series, **2697**(1), 012005 (2024). https://doi.org/10.1088/1742-6596/2697/1/012005
[6] V.R. Rasulov, R.Y. Rasulov, M.Kh. Nasirov, I.A. Muminov, and M.M. Mamatova, "Theory of size quantization in monolayers of transition metal dichalcogenides," Physica Scripta, **99**(10), 105987 (2024).
[7] E.I. Golant, and A.B. Pashkovskii, "Two-level electron wave functions in double-barrier quantum-confined structures in an electric field of finite amplitude," Semiconductors (Fizika i Tekhnika Poluprovodnikov), **34**(3), 334–339 (2000).
[8] E.I. Golant, and A.B. Pashkovskii, "Resonant transitions between split levels of triple-barrier nanostructures and prospects for their application in submillimeter-range devices," Semiconductors (Fizika i Tekhnika Poluprovodnikov), **36**(3), 330 (2002).
[9] A.B. Pashkovskii, "Parity and abrupt broadening of resonant levels in triple-barrier structures." JETP Letters, **82**(3–4) 228 (2005).
[10] V.F. Elesin, "High-frequency response of double-barrier nanostructures," Journal of Experimental and Theoretical Physics (JETP), **121**(4), 925–931 (2002).
[11] V.F. Elesin, "Resonant tunneling of electrons interacting with phonons," Journal of Experimental and Theoretical Physics (JETP), **123**(5), 1096–1111 (2005).
[12] V.F. Elesin, "Resonant tunneling and nonlinear response in a high-frequency field," Journal of Experimental and Theoretical Physics (JETP), **124**(2), 379–386 (2003).
[13] V.F. Elesin, and I.Yu. Kateev, "High-frequency properties of double-well nanostructures," Semiconductors (Fizika i Tekhnika Poluprovodnikov), **42**(5), 586–591 (2008).
[14] R.Y. Rasulov, V.R. Rasulov, K.K. Urinova, M.A. Mamatova, and B.B. Akhmedov, "Single and multiphoton optical transitions in atomically thin layers of transition metal dichalcogenides," East European Journal of Physics, (1), 393–397 (2024). https://doi.org/10.26565/2312-4334-2024-1-40
[15] V.R. Rasulov, R.Ya. Rasulov, M.A. Mamatova, and F. Qosimov, "Semiclassical theory of electronic states in multilayer semiconductors. Part 1," Journal of Physics: Conference Series, **2388**, 012156 (2022). https://doi.org/10.1088/1742-6596/2388/1/012156
[16] V. R. Rasulov, R.Ya. Rasulov, M.A. Mamatova, and F. Qosimov, "Semiclassical theory of electronic states in multilayer semiconductors. Part 2," Journal of Physics: Conference Series, **2388**, 012158 (2022). https://doi.org/10.1088/1742-6596/2388/1/012158
[17] T.P.E. Broekaert, W. Lee, and C.G. Fonstad, "Pseudomorphic $In_{0.53}$ $Ga_{0.47}As$/AlAs/InAs resonant tunneling diodes with peak-to-valley current ratios of 30 at room temperature," Applied Physics Letters, **53**(16), 1545–1549 (1988).
[18] S.-H. Ng, and C. Surya, "Studies of flicker noise in $In_{0.53}$ $Ga_{0.47}As$/AlAs/InAs resonant tunneling diodes," Solid-State Electronics, **35**(9), 1213–1216 (1992). https://doi.org/10.1016/0038-1101(92)90151-2
[19] D.J. BenDaniel, and C.B. Duke, "Space-charge effects on electron tunneling," Physical Review, **152**(2), 683–692 (1966). https://doi.org/10.1103/PhysRev.152.683
[20] G. Bastard, *Wave Mechanics Applied to Semiconductor Heterostructures*. Les Editions de Physique, Les Ulis (France); (Halsted Press, New York, 1988).

[21] V. Barsan, and M.C. Ciornei, "Semiconductor quantum wells with BenDaniel–Duke boundary conditions: approximate analytical results," European Journal of Physics, **38**(1), 015407 (2017). https://doi.org/10.1088/1361-6404/38/1/015407
[22] M. Singh, H. Lipsanen, T. Bhardwaj, and V. Singh, "Landau quantization of a circular quantum dot using the BenDaniel–Duke boundary condition," Superlattices and Microstructures, **147**, 106690 (2020). https://doi.org/10.1016/j.spmi.2020.106690
[23] A. Atić, X. Wang, N. Vuković, N. Stanojević, A. Demić, D. Indjin, and J. Radovanović, "Resonant tunnelling and intersubband optical properties of ZnO/ZnMgO semiconductor heterostructures: impact of doping and layer structure variation," Materials, **17**(4), 927 (2024). https://doi.org/10.3390/ma17040927
[24] R.Y. Rasulov, V.R. Rasulov, K.K. Urinova, I.A. Muminov, and B.B. Akhmedov, "Analysis of kinetic properties and tunnel-coupled states in asymmetrical multilayer semiconductor structures," East European Journal of Physics, (2), 270–273 (2024). https://doi.org/10.26565/2312-4334-2024-2-27
[25] R.Ya. Rasulov, V.R. Rasulov, I.A. Muminov, M.A. Mamatova, F.U. Raxmatullayeva, and M.Sh. Yusupova, "Electron states in a five-layer semiconductor structure. Part 1," East European Journal of Physics, (3), 491-497 (2026). https://doi.org/10.26565/2312-4334-2026-3-44

ЕЛЕКТРОННІ СТАНИ У П'ЯТИШАРОВИХ НАПІВПРОВІДНИКОВИХ СТРУКТУРАХ. ЧАСТИНА 2

Р.Я. Расулов, В.Р. Расулов, І.А. Мумінов, М.А. Маматова, Ф.У. Рахматуллаєва, С.Х. Мухаммадамінов
Ферганський державний університет, вул. Мураббійлар, 19, Фергана, 150100, Узбекистан

У роботі виведено та проаналізовано трансцендентні рівняння для визначення енергетичного спектра електронів у п'ятишаровій напівпровідниковій структурі з потенціальним бар'єром, розташованим у її центрі, для різних енергетичних діапазонів. Показано, що причина зміщення енергетичних рівнів пов'язана із залежністю гамільтоніана електрона не лише від потенціальної енергії, але й від кінетичної енергії, яка визначається ефективними масами електронів у кожному шарі структури. Проаналізовано зміни енергетичного спектра електронів у п'ятишаровій напівпровідниковій структурі, шари якої мають різні значення фізичних величин, що характеризують зонні та геометричні параметри зразка, залежно від температури.

Ключові слова: *п'ятишарова напівпровідникова структура; зв'язані квантові ями; потенціальний бар'єр; енергетичний спектр електронів; трансцендентні рівняння квантування; невідповідність ефективних мас; граничні умови Бастарда; температурна залежність; модель Кейна; резонансно-тунельні структури*